

# Multi-Label Noise Robust Collaborative Learning Model for Remote Sensing Image Classification

Ahmet Kerem Aksoy, *Student Member, IEEE*, Mahdyar Ravanbakhsh, *Member, IEEE*,  
and Begüm Demir, *Senior Member, IEEE*

**Abstract**—The development of accurate methods for multi-label classification (MLC) of remote sensing (RS) images is one of the most important research topics in RS. Methods based on Deep Convolutional Neural Networks (CNNs) have shown strong performance gains in RS MLC problems. However, CNN-based methods usually require a high number of reliable training images annotated by multiple land-cover class labels. Collecting such data is time-consuming and costly. To address this problem, the publicly available thematic products, which can include noisy labels, can be used to annotate RS images with zero-labeling cost. However, multi-label noise (which can be associated with wrong and missing label annotations) can distort the learning process of the MLC algorithm. The detection and correction of label noise are challenging tasks, especially in a multi-label scenario, where each image can be associated with more than one label. To address this problem, we propose a novel noise robust collaborative multi-label learning (RCML) method to alleviate the adverse effects of multi-label noise during the training phase of the CNN model. RCML identifies, ranks and excludes noisy multi-labels in RS images based on three main modules: 1) discrepancy module; 2) group lasso module; and 3) swap module. The discrepancy module ensures that the two networks learn diverse features, while producing the same predictions. The task of the group lasso module is to detect the potentially noisy labels assigned to the multi-labeled training images, while the swap module task is devoted to exchanging the ranking information between two networks. Unlike existing methods that make assumptions about the noise distribution, our proposed RCML does not make any prior assumption about the type of noise in the training set. The experiments conducted on two multi-label RS image archives confirm the robustness of the proposed RCML under extreme multi-label noise rates. Our code is publicly available online: <http://www.noisy-labels-in-rs.org>

**Index Terms**—Multi-label noise, collaborative learning, multi-label image classification, deep learning, remote sensing

## I. INTRODUCTION

REMOTE sensing (RS) images acquired by satellite-borne and airborne sensors are a rich source of information for monitoring the Earth surface, e.g., urban area studies, forestry applications, and crop monitoring [1]. As a result of recent advances in RS technology, huge amounts of RS images have been acquired and stored in massive archives, from which the mining of useful information is an important and challenging issue. Specifically, developing novel multi-label RS image scene classification methods that automatically assign multiple land-cover class labels (i.e., multi-labels) to each RS image scene in an archive is a growing research interest in RS. In

recent years, deep learning (DL) approaches have attracted great attention also in the multi-label classification (MLC) of RS images due to their high capability to describe the complex spatial and spectral content of RS images. As an example, in [2] convolutional neural networks (CNN) that contain the softmax function as the activation of the last CNN layer are presented. In [3], a radial basis function neural network with a multi-label classification layer is proposed. In [4], an attention-based long short-term memory (LSTM) network is used to sequentially predict classes one after another. An encoder-decoder neural network that includes: i) a squeeze excitation layer (which characterizes the channel-wise inter-dependencies of the image feature maps); and ii) an adaptive spatial attention mechanism (which models the informative image regions) is proposed in [5]. A multi-attention-driven approach that contains: i) spatial resolution-specific CNNs in a branch-wise architecture; and ii) a bidirectional LSTM network is presented in [6]. A study to analyze and compare different DL loss functions in the framework of MLC of RS images is recently presented in [7].

Most of the above mentioned DL-based approaches for the MLC of RS images require a sufficient number of high-quality (i.e., reliable) training images annotated with multi-labels. This is crucial for accurately characterizing complex content of images with discriminative and descriptive features and thus for achieving accurate multi-label predictions. However, the collection of a sufficient number of reliable multi-labeled images is time-consuming, complex and costly in operational scenarios and can significantly affect the final accuracy of the MLC methods [8]. To overcome this problem, a common approach is to employ DL models pre-trained on publicly available Computer Vision (CV) datasets (e.g., ImageNet [9]). Then, the pre-trained models are fine-tuned by considering a small set of multi-labeled RS images for the target classification task. This approach is not optimal for RS images due to different image characteristics in CV and RS (e.g., RGB images in CV compared to the Sentinel-2 multispectral images that contain 13 spectral bands associated with varying and lower spatial resolutions). In addition, the semantic content (and thus the considered semantic classes) present in RS images is significantly different from that of CV images (see Fig. 1). Thus, DL models trained from scratch on a large RS training set annotated with multi-labels are required. An effective approach for constructing a large training set with zero-annotation effort is to exploit the publicly available thematic products (e.g., the Corine Land Cover [CLC] map [10], the GLC2000 and the GlobCover) in RS as labeling sources

A. K. Aksoy, M. Ravanbakhsh, and B. Demir are with the Faculty of Electrical Engineering and Computer Science, Technische Universität Berlin, 10623 Berlin, Germany (emails: a.aksoy@tu-berlin.de, ravanbakhsh@tu-berlin.de, demir@tu-berlin.de).

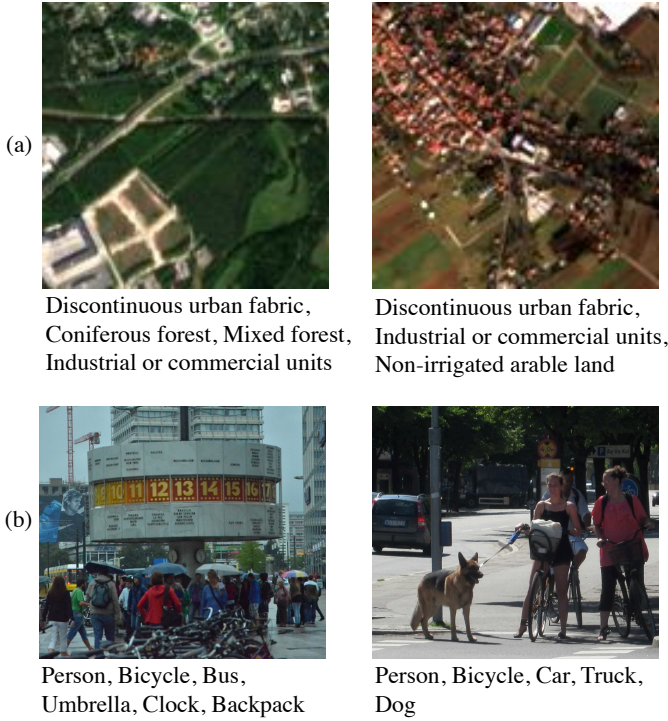


Fig. 1: An example of multi-labeled images (a) in RS [8]; and (b) in CV [15].

[8,11]. As an example, Sumbul et al. develop the BigEarthNet benchmark archive made up of Sentinel-2 multispectral images annotated by using the CLC map to drive the DL studies in RS MLC [8]. Constructing such large RS training sets with zero labeling cost is highly valuable. However, the set of land-use and land-cover class labels available in a given area through the thematic products can be incomplete or wrong (i.e., noisy). As an example, according to the validation report of the CLC, the accuracy is around 85% [12]. Using training images with noisy labels may result in uncertainty in the MLC model and thus may lead to reduced performance on multi-label prediction. Accordingly, methods that reduce the negative impact of noisy annotations are needed in the framework of RS MLC. When the training images are associated with multi-labels, two types of noise can exist for a given RS image:

- 1) Noise associated with missing labels: This type of noise appears when a land cover class label is not assigned to an image while that class is present in the image (i.e., the label is missed from the label set of that image) [13].
- 2) Noise associated with wrong labels: This type of noise appears when a land cover class label is assigned to an image although that class is not present in the given image (i.e., the label is wrongly assigned in the label set of that image) [14].

The number of missing or wrong class labels can vary depending on the labeling source. It is worth noting that the two types of noise can simultaneously appear associated to different spatial areas of a given RS image (e.g., a land-cover class label can be missed, while another land-cover class label is wrongly assigned in different spatial portions

of the image). Since DL models can easily overfit to noisy labeled data [16,17], dealing with label noise can significantly improve the MLC performance. Recently a couple of studies in RS are presented to learn from noisy labels in RS MLC. As an example, in [18], a semantic segmentation method that identifies label noise is presented to generate accurate land-cover maps by classifying RS images. This is achieved by simply evaluating the loss values since the noisy image labels are associated with the highest values of the loss. However, this method can only identify the wrong label noise and ignores the missing label noise problem. Hua et al. propose a regularization method to improve the MLC performance in RS under label noise [19]. The regularization is defined on the basis of a label correlation matrix, which is constructed by measuring the distances between corresponding word vectors in a text embedding space. Construction of a reliable label correlation matrix for different RS applications is a complex task due to the difficulty in collecting text descriptions of class labels for properly modeling the correlation between all possible combinations of classes present in RS images. The performance of these two methods depends on the accurate estimation of noise distribution in the considered data. Thus, there is a need to make prior assumptions about the noise type, which restricts the applicability and generalization capability of the methods for different MLC applications with different noise distributions. This is a critical limitation for complex RS MLC problems. Unlike RS, in the CV and multimedia communities, the development of noise robust DL models is much more extended and widely studied (see Sec. II-A for the literature survey). However, most of the existing methods assume that each image is annotated by a single label associated with the most significant content of the considered image [20,21]. Adapting single label noise tolerance methods for multi-labeled images is a challenging task due to the complexity of modeling the above-mentioned two types of noise in multi-labeled images. This becomes more critical when the number of land-cover classes (and thus class combinations) increases.

To address this problem, we propose a novel Robust Collaborative Multi-label Learning (RCML) method. Unlike the existing methods in the literature, the proposed method identifies, ranks and excludes samples with noisy multi-labels in RS images without making any prior assumption about the type of noise in the training set. To this end, the proposed RCML method contains three modules: 1) discrepancy module; 2) group lasso module; and 3) swap module. The discrepancy module aims at forcing the two networks to learn diverse features, while achieving consistent predictions. To automatically identify the noise type, we propose a group lasso module that computes a sample-wise ranking loss. The swap module exchanges the ranking information between the two collaborative networks and excludes extremely noisy labeled images from backpropagation. Our proposed collaborative learning method has been briefly introduced in [22], which was only applicable for training sets with a high noise rate. This paper extends the previous work by addressing the limitations of the earlier method and includes a detailed description of each step with an expanded experimental analysis. The main contributions of

this work are summarized as follows:

- To the best of our knowledge, RCML is the first method that automatically identifies the two types of noise in multi-labeled RS images without any prior assumption about the noise distribution.
- RCML can learn from highly noisy training sets by identifying the noisy samples and excluding them from the training process.
- We adapt a collaborative learning approach to be suitable for multi-labeled images based on ranking training images according to their identified label noise and exchanging this ranking information.
- The proposed RCML is an architecture-independent method, which can be integrated in different classification approaches.

The rest of the paper is organized as follows. In Section II we survey the DL based methods presented in the CV and multimedia communities for learning from noisy single-labeled and multi-labeled training images. In Section III, we introduce the proposed RCML method in detail. Section IV describes the considered datasets and the experimental setup, while Section V represents the experimental results. Finally, Section VI concludes the paper.

## II. RELATED WORK

In this section we review the methods that are robust to label noise and are presented in the CV literature in the context of image scene classification. We categorize the considered methods in two sub-sections as: 1) methods robust to noise on single-labeled images; and 2) methods robust to noise on multi-labeled images.

### A. Methods Robust to Noise on Single-Labeled Images

When an image is annotated by a single label, there is only one type of noise associated to the wrong class label assignment. The methods in this category aim to model the noise distribution present in the data considering only this type of noise to reduce the influence of noisy labels on the result. Patrini et al. propose a loss correction method by estimating the noise transition matrix of data [23]. This method aims at fixing the class-dependent label noise in the data, given the probability of each class being wrongly assigned into another. However, as the number of classes increases, it becomes harder to estimate the noise transition matrix, making the method difficult to scale. In [24], the correct labels are considered latent variables in the presence of noisy labels, and the expectation-maximization [25] algorithm is applied to iteratively calculate the correct labels as well as the network parameters. This scheme is also extended to scenarios, where noisy labels are dependent on the features, by modeling noise via a softmax layer that connects correct labels to noisy labels. In [26], it is shown that using the common overfitting prevention techniques (e.g., regularization and dropout) can be partially effective when dealing with label noise. However, in these cases, label noise may still affect the performance of the classifier, resulting in an accuracy drop. Moreover, since noise injection is already an overfitting prevention technique that

attempts to improve generalization performance [27], there is need to apply appropriate regularization to prevent underfitting of the classifier. In [28] an early-learning regularization (ELR) method is proposed to utilize the memorization effects of DL models. The ELR introduces a regularization term that aims to identify the more important parameters for learning the clean labels before early stopping, then deactivating the unimportant parameters to prevent the model fitting on noisy labels. Sukhbaatar et al. explore the performance of CNNs trained on noisy labels. CNNs are modified by including an additional fully connected layer at the end of their network architecture to adapt the predictions to the noisy label distribution of the data [29]. In [30], the training set is partitioned into multiple subsets to train multiple classifiers. If all classifiers agree on a label from the original training set, the label is updated with the agreed label prediction. This process is repeated over several stages, which gradually improve the overall performance. Nonetheless, this process depends on the performance of the individual classifiers, and it can take much time when large and complex training sets are used. Dehghani et al. use a student model that is trained on noisy data along with a teacher model that exploits the noise structure that is extracted by the student model [31]. However, this approach needs training samples with both clean and noisy labels, which is not always available.

In [32] a self-adaptive training (SAT) algorithm is proposed to dynamically correct noisy training samples. To this end, the SAT uses an exponential moving average of the model predictions to improve the generalization of deep networks under label noise. Similarly, in [33] a self-error-correcting CNN is proposed that can operate on completely noisy data. The network swaps potential noisy labels with the most probable prediction of the network, while simultaneously optimizing the model parameters. In [34] a simple strategy to separate the noisy labels from clean labels is introduced. This strategy employs a hard-sample mining technique based on Focal loss (FL) [35] to distinguish clean samples from noisy ones during the early stage of training. Failing to distinguish hard samples from noisy ones is a common problem when fixing labels, which may result in an undesired situation where the model swaps labels by mistake. To address this issue, Wu et al. use semantic bootstrapping to detect noisy samples and remove them from training [36]. Removing as few samples as possible is an important aspect of the noisy sample removal process to avoid unnecessary information loss. In [37] a deep neural network (DNN) is trained in an unsupervised fashion over a noisy training set by zero-weighting the noisy labels while keeping the samples in the training process. This prevents losing training samples, and thus allows DNNs to learn from more samples.

The idea of curriculum learning by using multiple networks has been exploited in MentorNet [38]. MentorNet imposes a data-driven sample weighting curriculum learning on the student network to choose clean samples from the data. Han et al. propose a learning paradigm called Co-Teaching [39], which we inspired our collaborative model based on. Under Co-Teaching, two networks are trained simultaneously, choosing batches that include only clean training samples to

feed each other. Each network back-propagates the mini-batch that is chosen by its peer network to update itself. Han et al. demonstrate that co-teaching is an effective method when dealing with label noise. In [40], the authors propose a co-teaching method with an additional discrepancy measurement to make the used networks diverge. The two peer networks that learn different features of the same probability distribution are used. Then, both networks select clean samples for each other based on their predictions to improve performances mutually. Ren et al. propose a meta-learning algorithm, in which a weighting factor is assigned to each training sample based on its gradient direction [41]. Although this method achieves impressive results, it needs a small set of clean training samples, which may not always be present. One of the advantages of the Co-Teaching methods is that they can be decoupled from the training process of any specific classifier. Such decoupled label noise estimation process allows Co-Teaching approaches to be used and tested with different network architectures. However, the success of the above-mentioned works mostly depends on the accurate estimation of noise distribution in data, which restricts the applicability and generalization capability of these methods.

### B. Methods Robust to Noise on Multi-Labeled Images

Most of the above-mentioned works are designed to address only one type of noise (i.e., wrong class label assignment) and thus it is not easy to simply extend or apply these methods in the framework of the MLC of RS images. There are also few works presented in the literature to address the multi-label noise problems. As an example, Ghosh et al. study different loss functions such as categorical cross-entropy (CCE), mean square error (MSE) and mean absolute error (MAE) for noise robust MLC, and argue that MAE is more robust to label noise compared to the others [42]. In [43], it is stated that MAE shows poor performance with more complex training sets, and a set of robust loss functions that combine CCE and MAE is proposed. This is known as noise robust alternative of CCE [42]. Meta-Learning and ensemble methods are other approaches proposed to address the label noise in MLC problems. Li et al. aim to find noise-tolerant model parameters using a teacher model along with a student model to make accurate predictions by optimizing a meta-objective, which encourages the student model to give consistent results with the teacher model after introducing synthetic labels [44]. Bucak et al. present a ranking-based multi-label learning method that exploits the group lasso to enhance the accuracy with missing class labels [45]. This method initially computes two error values: i) error associated with predicted classes in the multi-label set; and ii) error for the unpredicted ones within the same multi-label set for each sample. The two errors are then combined to define the ranking error for each unpredicted class. This error value indicates the possible missing class for the related sample. Finally, all the ranking errors associated with that sample are summed to define a final ranking error. The group lasso is introduced in [46] as an extension to the regular lasso, grouping a set of variables together for accurate prediction in regression. It is effective, because it groups

variables together to be included or excluded completely, as opposed to regular lasso, which only selects variables individually. The group lasso is used to regularize the network in [45], giving empirically robust results against missing class labels. Durand et al. propose a modified binary cross-entropy loss, which reduces the negative effects of missing class labels during training [14]. Jain et al. address the problem of missing class labels by defining a novel loss function called propensity scored loss (PSL) [13]. PSL can prioritize the most relevant labels over the many irrelevant ones and provide an unbiased estimation of the true labels without omitting the missing labels entirely.

As mentioned before, two types of noise (which are associated with wrong and missing class labels) may exist when training images annotated with multi-labels are considered. However, all the aforementioned methods are designed to overcome only one type of label noise in the training data (either missing or wrong class labels). Thus, these methods are not capable of identifying the two noise types simultaneously, which is an important limitation in MLC. In this paper to address this issue, we propose a novel collaborative learning method that aims at training a DL model robust to the two types of label noise based on a group lasso module without any prior assumption in the framework of MLC of RS images.

## III. PROPOSED METHOD

The proposed RCML method consists of three main modules: 1) discrepancy module; 2) group lasso module; and 3) swap module. The discrepancy module is devoted to allow the two networks that are used collaboratively in the method to learn different feature sets, while ensuring consistent predictions. The group lasso module aims at identifying potential noisy class labels by computing a sample-wise ranking loss and penalizing noisy labeled images. The swap module aims at exchanging the ranking information between the networks by using the ranking loss functions into consideration and excluding the detected noisy samples in the final loss calculation. RCML follows the principle of a collaborative framework called Co-Training to exchange ranking information between networks and to select samples associated with small loss values from the training set. Co-Training is a semi-supervised learning technique that was first proposed in [47] in order to overcome the labeled data insufficiency. Inspired by [40], we use two CNNs with the same architectures, which learn independent set of features, while attaining the same class distribution. Therefore, it becomes easier for the networks to find their potential faults. This improves the ability of selecting training images with clean labels immensely, since two networks are forced to learn different features and correct each other by exchanging their loss information. It is worth noting that, our proposed collaborative model is architecture-independent, since it does not rely on any specific network architecture. The RCML modules are applicable in the framework of any classification algorithm to detect the potentially noisy labels assigned to the training images with multi-labels.

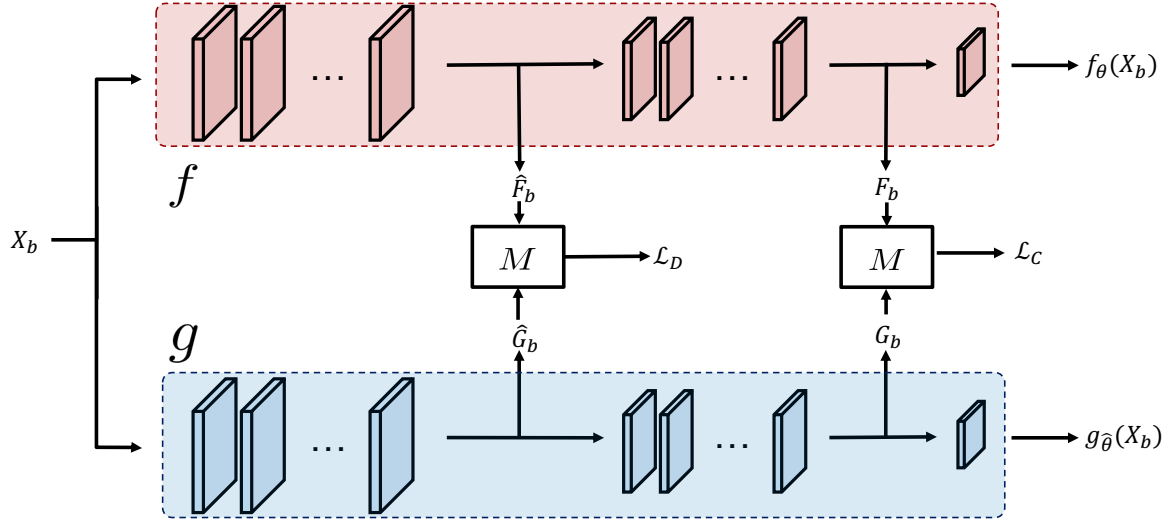


Fig. 2: Block diagram of the proposed discrepancy module.  $\mathbf{X}_b$  denotes the set of training images in the given mini-batch  $b$ .  $f$  and  $g$  represent the networks.  $\hat{F}_b$  and  $\hat{G}_b$  stand for the intermediate logits of the networks.  $F_b$  and  $G_b$  stand for the logits of the last layers.  $M$  is the discrepancy module.  $\mathcal{L}_D$  is the disparity loss, and  $\mathcal{L}_C$  is the consistency loss.

#### A. Problem Formulation

We consider a multi-label image classification problem with a training set  $\mathcal{D} = \{(\mathbf{x}_i, \mathbf{y}_i)\}_{i=1}^D$ , where  $\mathbf{x}_i$  denotes the  $i^{th}$  training image. Each training image is associated with one or more classes from a set of labels  $\{l_1, l_2, \dots, l_V\}$  where  $V$  is the total number of classes.  $\mathbf{y}_i = [y_i^v]_{v=1}^V \in \{0, 1\}^V$  is a binary vector, where  $y_i^v$  indicates the presence or absence of  $v$ -th label for the image  $\mathbf{x}_i$ . We assume that the labels in  $\mathbf{y}_i$  can be noisy (e.g., wrong or missing). To reduce the adverse effect of a noisy label, we propose a novel robust collaborative multi-label learning (RCML) method, based on two collaborative CNNs. In detail, we use two CNNs with identical architectures that are represented as  $f$  and  $g$  with parameters  $\theta$  and  $\hat{\theta}$ , respectively. Loss functions  $\mathcal{L}_f$  and  $\mathcal{L}_g$  are the classification loss functions for networks  $f$  and  $g$ , respectively. For each network, the Binary Cross Entropy (BCE) is chosen for the classification loss function as suggested in [8]. The considered collaborative networks aim at: i) learning diverse features, while producing the consistence class predictions; and ii) being capable of correcting errors of each other during the training through information exchange. To this end the proposed RCML contains three main modules: 1) discrepancy module; 2) group lasso module; and 3) swap module. Each module is described in details the following sub-sections.

#### B. Discrepancy Module

In a collaborative learning framework, the networks must learn independent features while predicting the same class distribution. The networks are required to be capable of fixing mistakes of each other in the training process by exchanging information. If they do not learn diverse features on the same mini-batch, they cannot enhance predictions with each other mutually. To achieve the desired diversity, we propose a discrepancy module embedded in our method, which includes two loss functions: i) the disparity loss ( $\mathcal{L}_D$ ); and ii) the

consistency loss ( $\mathcal{L}_C$ ). The disparity loss function ensures that the networks learn distinct features, while the consistency loss function ensures that the two networks produce similar predictions. Therefore, for each mini-batch  $b$  the disparity loss is calculated between the chosen layers of the networks, and the consistency loss is calculated at the end of the networks (See Fig. 2). The disparity loss  $\mathcal{L}_D$  is defined as:

$$\mathcal{L}_D = M(\hat{\mathbf{F}}_b, \hat{\mathbf{G}}_b), \quad (1)$$

$$\hat{\mathbf{G}}_b = g_{\hat{\theta}(1:c)}(\mathbf{X}_b), \hat{\mathbf{F}}_b = f_{\theta(1:c)}(\mathbf{X}_b),$$

where  $M$  is the discrepancy module.  $\hat{\mathbf{F}}_b$  and  $\hat{\mathbf{G}}_b$  represent the logits of the layers before the module. The parameters of the networks  $f$  and  $g$  up to the layer  $c$  denoted as  $\theta(1:c)$  and  $\hat{\theta}(1:c)$ , respectively.  $c$  is the layer that the discrepancy module for the disparity loss is inserted. The set of training images in the given mini-batch  $b$  is denoted as  $\mathbf{X}_b$ . The consistency loss  $\mathcal{L}_C$  is defined as:

$$\mathcal{L}_C = M(\mathbf{F}_b, \mathbf{G}_b), \quad (2)$$

where  $\mathbf{F}_b$  and  $\mathbf{G}_b$  denote the logits of the last layer of the networks. The discrepancy module is a statistical distance function, which measures the difference between two probability distributions. In general, for the discrepancy module  $M$  any statistical distance function can be used (e.g., Maximum Mean Discrepancy (MMD) [48], and Wasserstein metric [49]). We select the MMD algorithm to be used in the discrepancy module due to its success to disentangle probability distributions [40]. The MMD is defined as the distance between the mean embeddings of the distributions in Reproducing Kernel Hilbert Space (RKHS) [50]. Formally, MMD for two distributions  $P$  and  $Q$  is defined as:

$$MMD(P, Q) = \|\mu_P - \mu_Q\|_H, \quad (3)$$

where  $\mu_P$  and  $\mu_Q$  denote the mean values of the distributions  $P$  and  $Q$ , respectively.  $H$  denotes the RKHS and  $\|\cdot\|_H$  repre-



sents the  $L_1$  norm. An empirical estimation of MMD between  $P$  and  $Q$  can be denoted as:

$$MMD(P, Q) = \frac{1}{m^2} \left[ \sum_{i=1}^m \sum_{t=1}^m k(\mathbf{s}_i^P, \mathbf{s}_t^P) - 2 \sum_{i=j}^m \sum_{t=1}^m k(\mathbf{s}_j^P, \mathbf{s}_t^Q) + \sum_{j=1}^m \sum_{t=1}^m k(\mathbf{s}_i^Q, \mathbf{s}_t^Q) \right], \quad (4)$$

where  $\mathbf{s}_j^P$  and  $\mathbf{s}_j^Q$  are  $j$ -th samples from respective distributions.  $k$  is the Gaussian radial basis function kernel [51].

### C. Group Lasso Module

The BCE loss function is a widely used objective function in multi-label learning. However, while training set contains label noise, the networks may be biased toward noise in the training set and perform poorly. Thus, an additional mechanism is necessary to avoid the model misguided by noisy training sets. The additional mechanism can have many forms, such as regularization, noisy labeled image exclusion, or noise correction. Inspired by [45], we introduce a ranking error function capable of dealing with two types of noise in a multi-label training set (missing label and wrong label) without considering prior assumption. To this end, the ranking error function for missing class labels proposed in [45] is extended to identify the wrong class label assignments as well. In addition, we do not use our ranking error function as a regularizer. Instead, we use it to detect noisy labels within a mini-batch and exclude them in the backpropagation. Excluding the training images with noisy labels in the backpropagation prevents overfitting to noisy training samples. The motivation behind using group lasso is to identify potential noisy labels in training set, given the opportunity to learn from those samples. Furthermore, it provides information about label noise type. Let  $\mathcal{E}_{l,\hat{l}}^f$  denote the ranking error function for network  $f$ :

$$\mathcal{E}_{l,\hat{l}}^f(\mathbf{x}_i) = \max \left( 0, [2(f_l(\mathbf{x}_i) - f_{\hat{l}}(\mathbf{x}_i)) + 1] \right), \quad (5)$$

where  $l \in L$  and  $\hat{l} \in \hat{L}$  denote the assigned and unassigned labels to the image  $\mathbf{x}_i$ , respectively.  $f_l(\mathbf{x}_i)$  and  $f_{\hat{l}}(\mathbf{x}_i)$  denote the prediction probabilities from network  $f$  for the classes  $l$  and  $\hat{l}$ , respectively. The ranking error function gives a measure of potential noise in a class combination. In the case of a clean prediction the ranking error is equal to 0, otherwise, the ranking error function returns a positive value indicating a label noise. The values from ranking error functions are gathered by two loss terms using the group lasso to identify the potential label noise. The ranking loss for network  $f$  defined as:

$$Lasso_f(\mathbf{x}_i) = \alpha \sum_{\hat{l} \in \hat{L}} \sqrt{\sum_{l \in L} \mathcal{E}_{l,\hat{l}}^2(\mathbf{x}_i)} + \beta \sum_{l \in L} \sqrt{\sum_{\hat{l} \in \hat{L}} \mathcal{E}_{l,\hat{l}}^2(\mathbf{x}_i)}, \quad (6)$$

where the first loss term calculates an aggregated loss based on missing class labels, while the second term calculates an aggregated loss for wrong class label assignments. This approach

allows our method to rank training samples associated with noisy labels according to their estimated noise rate and noise type by adjusting the importance factors ( $\alpha$  and  $\beta$ ) of the loss terms. Similarly, for network  $g$  the ranking loss  $Lasso_g(\mathbf{x}_i)$  is computed analogous to  $Lasso_f(\mathbf{x}_i)$ . Then, the calculated ranking losses obtained from each network are sent to the swap module to identify the training samples associated with noisy labels.

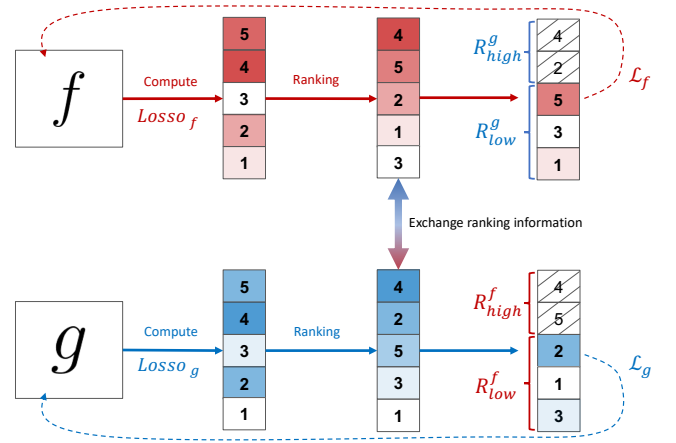


Fig. 3: A qualitative example to describe the swap module. The two networks  $f$  and  $g$  exchange the ranking information. Network  $f$  updates its weights by calculating final loss  $\mathcal{L}_f$ , using the samples with smaller ranking loss values  $R_{low}^g$  that are identified by  $g$ . Similarly, network  $g$  updates its parameters by calculating final loss  $\mathcal{L}_g$  wrt  $R_{low}^f$  identified by  $f$  from backpropagation. For this qualitative example, network  $f$  calculates the final loss as  $\mathcal{L}_f = \lambda_1 \mathcal{L}_{clc}(\{\mathbf{x}_1, \mathbf{x}_3, \mathbf{x}_5\}) + \lambda_2 \mathcal{L}_C - \lambda_3 \mathcal{L}_D$  to update its parameters.

### D. Swap Module

As shown in Fig. 3, the swap module is injected between the two collaborative networks and aims at exchanging the ranking information obtained from the group lasso module. In detail, the swap module uses the ranking losses calculated by (6) and sorts them by the ascending order. Then, the swap module splits the obtained ranking losses from each collaborative network into two sets: i) samples associated with highest ranking loss values ( $R_{high}^f$  and  $R_{high}^g$ , for networks  $f$  and  $g$ , respectively); and ii) samples associated with smaller ranking loss values ( $R_{low}^f$  and  $R_{low}^g$ , for  $f$  and  $g$ , respectively). Then the ranking information of samples associated with the highest and lowest loss values are exchanged between the two networks. To calculate the final loss for each network, the classification loss is only computed for the samples associated with lowest ranking loss values (i.e., identified samples with clean labels). In detail, network  $f$  calculates the final loss  $\mathcal{L}_f$  by using  $R_{low}^g$  identified by the network  $g$ , and vice versa. A visualization of the process is illustrated in Fig. 3. The final losses for two networks  $f$  and  $g$  are defined as:

$$\begin{aligned} \mathcal{L}_f &= \lambda_1 \mathcal{L}_{clc}(\mathbf{x}_r^g) + \lambda_2 \mathcal{L}_C - \lambda_3 \mathcal{L}_D, \forall \mathbf{x}_r^g \in R_{low}^g, \\ \mathcal{L}_g &= \lambda_1 \mathcal{L}_{clc}(\mathbf{x}_r^f) + \lambda_2 \mathcal{L}_C - \lambda_3 \mathcal{L}_D, \forall \mathbf{x}_r^f \in R_{low}^f, \end{aligned} \quad (7)$$

where  $\lambda_1$  is a weight value for the BCE loss calculated over the identified samples associated with the lowest ranking loss values.  $\lambda_2$  and  $\lambda_3$  represent the weights for  $\mathcal{L}_C$  and  $\mathcal{L}_D$ , respectively. The number of samples associated with smaller ranking loss (i.e.,  $R_{low}^g$  and  $R_{low}^f$ ) is defined by an adaptive parameter swap rate  $\gamma$ . The swap rate indicates the contribution of the identified clean samples in the final loss value. It worth noting that the disparity loss  $\mathcal{L}_D$  forces two networks learn distinct features, therefore it is maximized. The consistency loss  $\mathcal{L}_C$  is minimized to ensure that the networks produce similar predictions. Through an end-to-end training of the two collaborative networks the parameters of the networks  $f$  and  $g$  are learned by minimizing the  $\mathcal{L}_f$  and  $\mathcal{L}_g$  losses, respectively. After the training phase, both networks are used to classify each image in the archive.

#### IV. DATASET DESCRIPTION AND EXPERIMENTAL SETUP

##### A. Dataset Description

We conducted experiments on two different benchmark RS datasets. The first dataset is the Ireland subset of the BigEarthNet (denoted as IR-BigEarthNet) benchmark archive [8], which consists of 15894 Sentinel-2 multispectral images acquired between June 2017 and May 2018 over Ireland. Each image was annotated by multiple land-cover classes provided by 2018 CORINE Land Cover Map (CLC) inventory. Sentinel-2 images contain 13 spectral bands with varying spatial resolutions. Each image in IR-BigEarthNet is a section of: i)  $120 \times 120$  pixels for the bands that have a spatial resolution of 10m; ii)  $60 \times 60$  pixels for the bands that have a spatial resolution of 20m; and iii)  $20 \times 20$  pixels for the bands that have a spatial resolution of 60m. In the experiments, we used the bands with 10m and 20m spatial resolutions (and thus 10 bands per image is used in total), excluding the two 60m bands due to their very low spatial resolution and small pixel size. The cubic interpolation was applied to 20m bands of each image to have the same pixel sizes associated with each band. In the experiments, we exploited the 19 land-cover class nomenclature proposed in [52] for BigEarthNet and eliminated 7 classes which are represented with a significantly small number of images in the dataset, leading to 12 classes in total. The number of labels associated with each image varies between 1 and 7, while 97.4% of images contain less than 5 labels. IR-BigEarthNet was divided into a validation set of 3839 images, a test set of 3856 images, and a training set of 8192 images. In the experiments, the images that are fully covered by seasonal snow, cloud and cloud shadow were not used as suggested in [8]. An example of images from IR-BigEarthNet together with their multi-labels is given in Fig. 4. Table I shows the number of training, validation and test samples associated to each considered class in IR-BigEarthNet.

The second dataset is the UC Merced Land Use (denoted as UCMerced) archive that consists of 2100 images selected from aerial orthoimagery and downloaded from the USGS National Map of the following US regions: Birmingham, Boston, Buffalo, Columbus, Dallas, Harrisburg, Houston, Jacksonville, Las Vegas, Los Angeles, Miami, Napa, New York, Reno, San

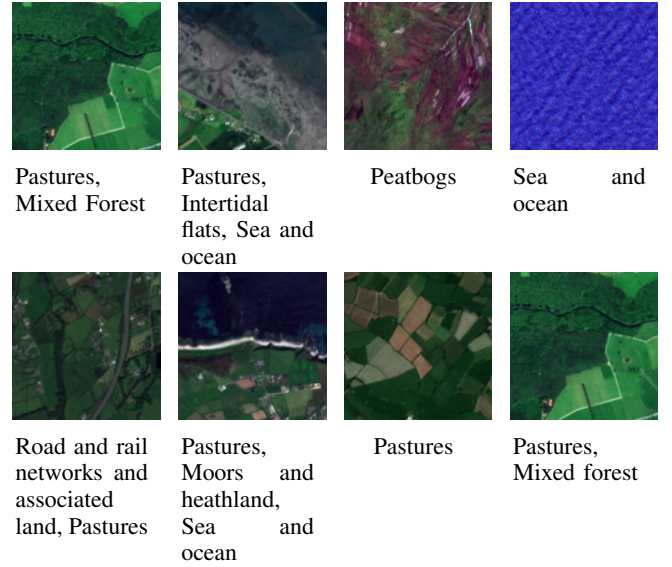


Fig. 4: An example of images with their multi-labels from the IR-BigEarthNet dataset.

TABLE I: Number of samples per class in training, validation and test sets of the IR-BigEarthNet dataset.

Class	Train	Val	Test
Urban fabric	818	369	371
Arable lands	2860	1404	1397
Pastures	5723	2725	2739
Complex cultivation patterns	510	240	226
Land principally occupied by agriculture, with significant areas of natural vegetation	896	420	414
Broad-leaved forest	410	205	199
Coniferous forest	1156	545	524
Mixed forest	588	273	296
Moors, heathland and sclerophyllous vegetation	467	217	219
Transitional woodland, shrub	708	345	369
Inland wetlands	811	400	415
Marine waters	2087	894	900

Diego, Santa Barbara, Seattle, Tampa, Tucson, and Ventura [53]. Each image is of size  $256 \times 256$  pixels and has a spatial resolution of 30m. In the experiments, we used the multi-label annotations of UCMerced images that were obtained based on visual inspection [54]. The total number of class labels is 17, while the number of labels associated with each image varies between 1 and 7. The number of training, validation and test samples in the multi-label UCMerced dataset is given in Table II. Fig. 5 shows an example of images together with their associated multi-labels from the UCMerced dataset.

##### B. Experimental Setup

In the experiments, we used ResNet [55] as a backbone for the proposed RCML. Among different versions of ResNet, each of which includes different numbers of layers, ResNet50 with 50 layers was chosen. Moreover, we used the improved residual units [56] that enhance the network's generalization performance and make training easier by introducing additional non-linearities. We utilized the SGD optimizer with an initial learning rate of  $10^{-3}$ . We used a learning rate scheduler

TABLE II: Number of samples per class in training, validation and test sets of the multi-label UCMerced dataset.

Class	Train	Val	Test
Airplane	70	15	15
Bare Soil	506	103	109
Buildings	482	102	107
Cars	631	125	130
Chaparral	77	21	17
Court	73	16	16
Dock	70	15	15
Field	73	15	15
Grass	683	145	147
Mobile home	70	17	15
Pavement	917	189	194
Sand	210	43	41
Sea	70	15	15
Ship	70	16	16
Tanks	70	15	15
Trees	702	155	152
Water	142	31	30

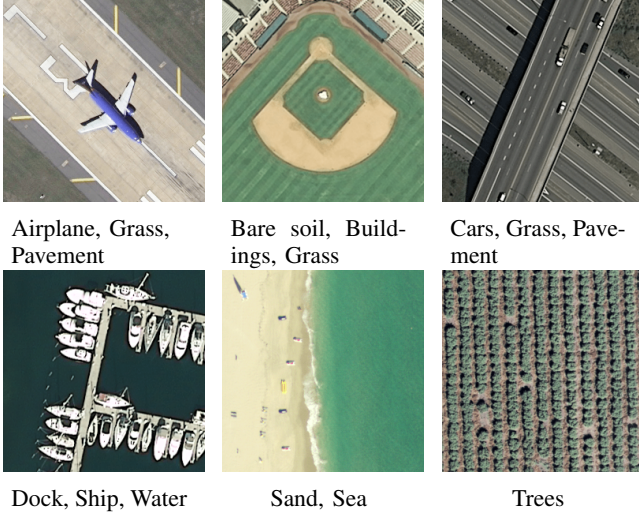


Fig. 5: An example of images with their multi-labels from the multi-label UCMerced dataset.

with an exponential decay rate of 0.9. The batch sizes for IR-BigEarthNet and multi-label UCMerced were set to 256 and 64, respectively. We report the results of training obtained after 100 epochs. The model training and further experiments were conducted on a Tesla V100 GPU with 32 GB RAM.

To identify the potential noisy samples, a ranking loss value for every sample was calculated by using the group lasso module. The group lasso has two parameters  $\alpha$  and  $\beta$  that control the effects of two different noise types on the calculation of the ranking loss. We define  $\beta = 1 - \alpha$ . A group lasso module with a higher  $\alpha$  concentrates more on finding the missing class labels, whereas a higher  $\beta$  gives a higher weight to detect the wrong class labels. Since we do not consider any prior assumption, the values of  $\alpha$  and  $\beta$  were set to 0.2 and 0.8, respectively based on a grid search strategy.

Within the swap module of the proposed RCML method, the networks exchange the calculated ranking information with each other. According to the ranking information, each network chooses a certain amount of samples (wrt the swap rate  $\gamma$ ) associated with the smaller ranking loss values iden-

tified from the other network to update its weights. For each mini-batch the identified samples associated with the highest ranking loss values are excluded from the final loss calculation. The goal of this process is to reduce the effect of noisy samples in backpropagation. Finding an appropriate value for the swap rate  $\gamma$  is not easy, since it is highly related to the noise rate in the training set [40]. Therefore, we exploit an adaptive weighting strategy to find an appropriate value for  $\gamma$ . In detail, the value of swap rate is determined based on the approximated noise rate ( $\hat{n}r$ ) through cross-validation over the validation set, and we set the swap rate to  $\gamma = 1 - \hat{n}r$ .

$y_1$	1	0	0	0	0	0	1	1	0	0
$y_2$	0	0	0	1	0	1	0	0	1	0
$y_3$	1	1	0	0	1	0	0	1	1	0
$\vdots$	1	1	0	1	0	1	0	0	1	0
$\vdots$	0	1	0	0	1	1	0	0	0	1
$\vdots$	0	0	0	1	0	1	0	0	1	0

Fig. 6: The considered label noise injection approach: Random Noise per Sample (RNS) with a sampling rate 0.5 and class rate of 0.5. The colored cells represent the introduced artificial label noise. Cells in blue represent “0” value in ground truth labels that are flipped to “1”, while those in red represent “1” value in ground truth labels that are flipped to “0”.

To verify the effectiveness of the proposed method, we added synthetic noise to the labels of the IR-BigEarthNet and multi-label UCMerced datasets. To ensure that both types of label noise (missing label and wrong label) are introduced to the multi-label training set, we designed a label noise injection approach called Random Noise per Sample (RNS). RNS chooses labels randomly from the training set by a predefined percentage called the sampling rate. Afterward, to apply noise, RNS randomly flips a certain number of selected labels. The number of flipped labels driven by a parameter called as class rate. An illustration of the considered label noise injection approach is shown in Fig. 6. The figure shows an example scenario for RNS with a sampling rate of 0.5 and a class rate of 0.5. Three samples out of six are selected, and label noise is randomly applied to half of their labels. In our experiments, the ratio of the introduced noise was varied from 0% to 50%. The results of the experiments were provided in terms of two main performance metrics averaged over three runs for each experiments: 1) mean average precision (mAP) with the micro and macro averaging strategy; and 2)  $F_1$  score with the micro averaging strategy. For an explanation of these metrics, the reader is referred to [6]. Since the proposed RCML includes two networks that run simultaneously, the network with the best mAP micro validation score has been chosen for evaluation. To further study the performance and the behavior of the proposed RCML, the class-based mAP scores are reported in comparative plots. We compared our proposed method with four baseline methods: 1) focal loss (FL) [35]; 2) self-adaptive training (SAT); 3) early-learning regularization (ELR) [28]; and 4) standard binary cross-entropy (BCE). To have a fair comparison for all the methods, we select the same



architecture (ResNet50) pre-trained on ImageNet under the same hyperparameters.

## V. EXPERIMENTAL RESULTS

### A. Sensitivity Analysis

This sub-section presents the sensitivity analysis results for the proposed RCML method under different values of the hyperparameters. In the group lasso module, the two hyperparameters  $\alpha$  and  $\beta$  are the weights for balancing the missing and wrong class label ranking losses, respectively. For the sensitivity analysis, we choose  $\alpha$  from a set of fixed values  $\alpha = [0.2, 0.5, 0.8]$ , while  $\beta = 1 - \alpha$ . We observe that  $\alpha$  and  $\beta$  are sensitive to: 1) the distribution of absence and presence classes in the label set (e.g., in our case, the majority of the class label for a given sample is absent); 2) the type of multi-label noise in the training set (e.g., missing label, or wrong class label). In the case of the availability of prior knowledge about the type of noise or class label distribution, we can use this prior to adjusting  $\alpha$  and  $\beta$ . In detail, a group lasso module with a higher value for  $\alpha$  weighs more on finding the missing class labels, whereas a higher  $\beta$  gives more weight to identifying the wrong class labels. Table III shows the sensitivity analysis results for  $\alpha$  and  $\beta$  for a low (10%) and high (40%) injected noise rate. From the table, one can observe that the wrong class label is more harmful than a missing class label since increasing  $\beta$  (the importance of noise in wrong class labels) improves the performance of the model. Thus, we set  $\alpha$  to 0.2 and  $\beta$  to 0.8. Also, by analyzing the results in Table III one can see that the proposed RCML is robust to the variations in  $\alpha$  and  $\beta$  for two different noise rates.

TABLE III: Sensitivity Analysis: The effect of the different values of  $\alpha$  and  $\beta$  on the mAP macro scores (%) under 10% and 40% injected noise rates on multi-label UCMerced dataset.

injected noise rate	10%			40%		
$\alpha$ ( $\beta=1-\alpha$ )	0.2	0.5	0.8	0.2	0.5	0.8
mAP macro (%)	<b>89.2</b>	88.7	89.0	<b>83.3</b>	80.7	81.4

The effect of different values for the hyperparameters  $\lambda_2$  and  $\lambda_3$  can be found in Table IV. The table reveals that when  $\lambda_2$  and  $\lambda_3$  are weighted equally, decreasing the value of these hyperparameters affects the performance of the proposed RCML negatively. As an example, when the value of  $\lambda_2$  and  $\lambda_3$  is set to 0.01, the mAP macro score drops by 2%. Furthermore, choosing a higher value for  $\lambda_2$  compared to  $\lambda_3$  outperforms the case where the value of  $\lambda_3$  is higher than  $\lambda_2$ . This shows that learning diverse features has a positive effect on the performance of the RCML. It is also observed that weighting both  $\lambda_2$  and  $\lambda_3$  equally with bigger values does not increase the performance.

### B. Ablation Study

To analyze the influence of each module, we designed different configurations by excluding individual modules from

TABLE IV: Sensitivity Analysis: The effect of the different values of  $\lambda_2$  and  $\lambda_3$  on the mAP macro score (%) of RCML for various settings (using multi-label UCMerced dataset with a noise rate of 40%).

$\lambda_2$	$\lambda_3$	mAP macro (%)
1.0	1.0	81.6
<b>1.0</b>	<b>0.1</b>	<b>83.3</b>
0.1	1.0	79.5
0.5	0.5	80.7
0.1	0.1	80.3
0.01	0.01	79.6

TABLE V: Ablation study: The effect of each module of the proposed RCML on the mAP macro scores (%) under 10% and 40% injected noise rates on multi-label UCMerced dataset.

Injected noise rate	10%	40%
RCML all modules	<b>89.2%</b>	<b>83.3%</b>
RCML without MMD	89.1%	82.6%
RCML without group lasso	89.2%	77.0%
RCML without swap	89.0%	81.4%
Standard CCML	82.1%	81.2%

the proposed RCML over the UCMerced dataset. Furthermore, we compared RCML with the standard CCML [22]. The standard CCML includes all modules of RCML and a flipping module that flips the noisy labels identified by both networks during the final training epochs. In detail, we compared RCML with the standard CCML and three different configurations of RCML when we exclude: 1) the MMD module; 2) the group lasso module; 3) the swap module. When removing the MMD module in the first configuration setup, there is no explicit objective to enforce two networks to learn different representations. In the second setup, to analyze the effect of the group lasso module, we use random sample selection instead of using the group lasso ranking information. When we remove the swap module, the two collaborative networks do not exchange the ranking information; instead, they update individually.

The results of the ablation study are presented in Table V in terms of mAP macro scores when the injected noise rates are 10% and 40%. The table shows that mAP obtained by RCML when including all the modules is the highest. We also observe that the MMD module has no intense influence on the mAP. However, it is necessary to include MMD to ensure that two networks learn different representations and the obtained representations are not identical. Furthermore, the group lasso module has its biggest impact when the noise rate increases. When the injected noise rate is high (i.e., 40%), the ranking information obtained from group lasso is crucial to identify the noisy samples correctly, rather than a random exclusion. The other important module is the swap module, which aims to exchange the ranking information between two collaborative networks. When we exclude this module, each network is trained independently from the other network, which increases

TABLE VI:  $F_1$ , mAP micro and mAP macro scores obtained by the proposed RCML, FL, SAT, ELR and BCE in IR-BigEarthNet dataset under different noise rates.

Noise Rate	$F_1$ (%)					mAP micro (%)					mAP macro (%)				
	FL	SAT	ELR	BCE	RCML	FL	SAT	ELR	BCE	RCML	FL	SAT	ELR	BCE	RCML
0%	64.0	66.0	66.2	<b>72.5</b>	72.3	78.5	77.6	80.6	<b>81.0</b>	80.9	45.5	43.8	47.7	49.6	<b>49.8</b>
10%	62.4	65.0	65.2	71.0	<b>72.3</b>	77.8	76.6	<b>80.1</b>	79.2	79.7	45.1	43.0	47.0	47.5	<b>47.8</b>
20%	55.9	62.4	62.3	67.9	<b>71.7</b>	77.3	74.4	79.0	77.4	<b>79.2</b>	43.8	41.0	45.5	45.5	<b>47.2</b>
30%	48.5	56.2	57.0	61.4	<b>70.8</b>	76.6	71.2	77.6	75.4	<b>79.0</b>	42.7	38.3	43.6	42.8	<b>46.6</b>
40%	39.0	48.3	48.4	56.3	<b>70.3</b>	75.6	69.0	76.0	76.5	<b>79.0</b>	40.7	36.0	41.4	41.7	<b>46.5</b>
50%	30.7	34.0	35.1	37.5	<b>67.8</b>	70.1	69.3	72.8	73.7	<b>78.5</b>	35.3	34.2	37.3	37.9	<b>45.3</b>

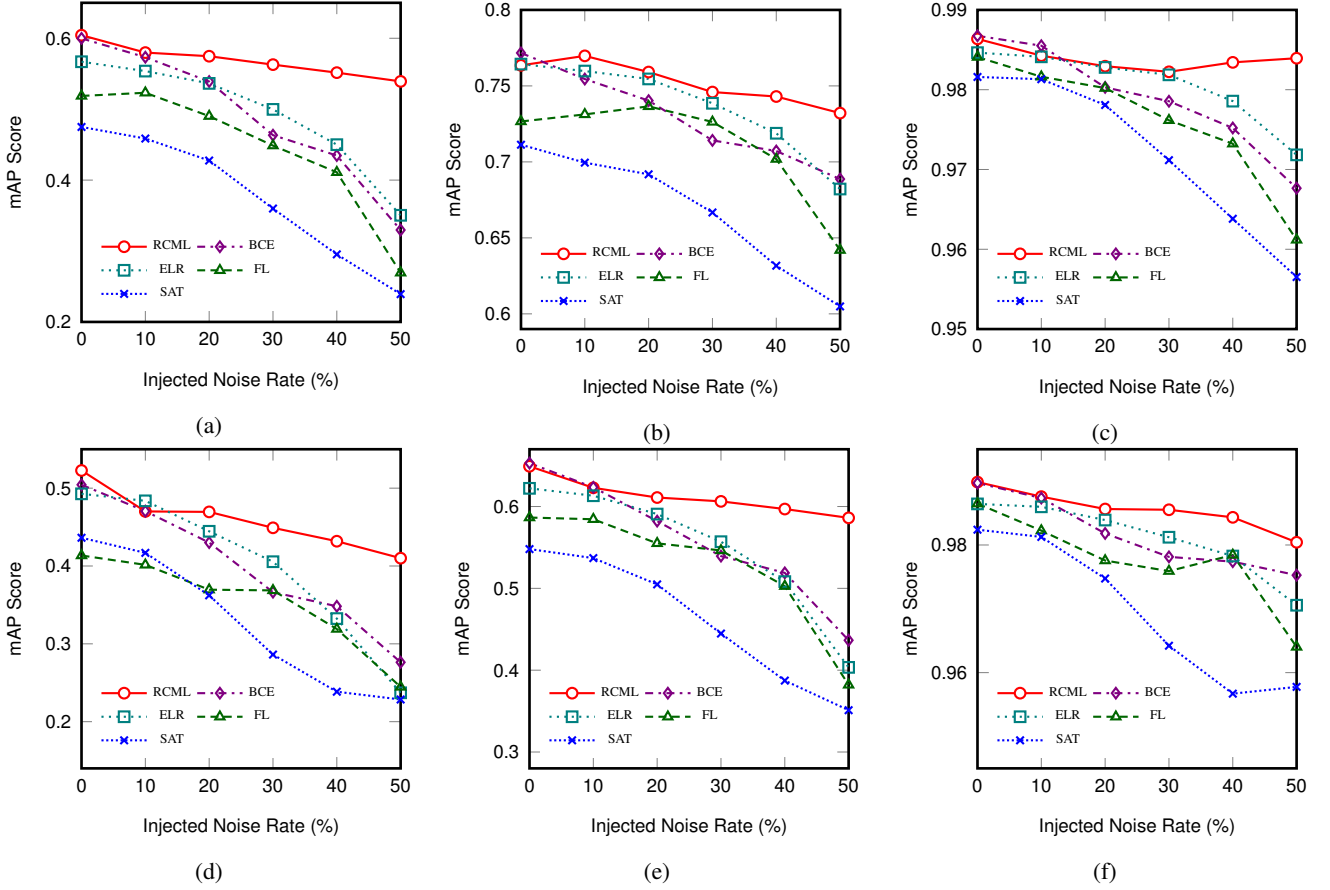


Fig. 7: Class-based comparison: Class-based mAP scores for different noise rates obtained by the proposed RCML, BCE, ELR, FL and SAT for six selected classes: (a) Urban fabric; (b) Arable lands; (c) Pasture; (d) Moors, heathland and sclerophyllous vegetation; (e) Inland wetlands; and (f) Marine waters in the IR-BigEarthNet dataset.

the risk of overfitting the noise since there is no consensual signal from the other network for correction. This becomes more severe when the noise rate is high, and learning process of the network(s) may distort with such a high noise rate in the multi-labels.

We also include the standard CCML to study the effect of improvements we made. The main drawback of the standard CCML is excluding a fixed portion of samples in each mini-batch (i.e.,  $\gamma=25\%$ ) from backpropagation regardless of the injected noise rate. This can severely reduce classification accuracy when the injected noise rate is low (e.g., less than 20%) since having a fixed swap rate  $\gamma=25\%$  excludes 25%

of the clean samples from backpropagation. We address this issue within the RCML by introducing an adaptive swap rate selection. RCML estimates the noise rate in the training set via cross-validation, and sets the swap rate accordingly. As an example, when the noise rate is 10% the standard CCML excluded 25% of the samples and obtained an mAP macro score of 82.1%, while RCML adaptively changes the swap rate to use all the clean samples and achieved 89.3%.

### C. Results on Multi-Label IR-BigEarthNet Dataset

The results on the IR-BigEarthNet are presented in Table VI. By analyzing the results in Table VI, one can see that

TABLE VII:  $F_1$ , mAP micro and mAP macro scores obtained by the proposed RCML, FL, SAT, ELR and BCE in the multi-label UCMerced dataset under different noise rates.

Noise	$F_1$ (%)					mAP micro (%)					mAP macro (%)				
Rate	FL	SAT	ELR	BCE	RCML	FL	SAT	ELR	BCE	RCML	FL	SAT	ELR	BCE	RCML
0%	78.8	80.2	79.1	<b>83.4</b>	83.3	85.1	86.8	90.2	90.8	<b>91.1</b>	81.3	83.4	89.3	<b>90.0</b>	89.8
10%	78.2	79.9	78.5	<b>83.1</b>	<b>83.1</b>	84.5	86.3	89.9	90.5	<b>90.7</b>	80.3	82.6	89.0	<b>89.5</b>	89.2
20%	74.4	77.2	74.1	82.4	<b>82.7</b>	81.3	83.7	88.8	88.8	<b>89.4</b>	76.1	78.8	87.5	86.7	<b>87.6</b>
30%	67.3	70.6	64.0	79.0	<b>82.1</b>	75.3	78.5	86.1	85.4	<b>88.6</b>	67.4	71.1	82.6	80.3	<b>85.7</b>
40%	60.7	63.8	55.2	74.4	<b>80.4</b>	69.0	73.0	83.0	81.8	<b>87.3</b>	59.5	63.9	77.8	74.5	<b>83.3</b>
50%	50.0	51.8	44.3	62.6	<b>78.2</b>	54.6	59.0	73.2	70.3	<b>85.5</b>	45.2	48.2	64.2	60.5	<b>79.4</b>

the proposed method outperforms the compared methods in all of the evaluation metrics over most of the injected noise rates. Under a noise-free training set (0% injected noise rate), RCML obtained comparable scores to the baseline BCE, while surpassing all of the state-of-the-art noise robust methods. As an example, BCE obtained  $F_1$  score 83.4%, while RCML and SAT obtained 83.3% and 80.2%, respectively. The results in Table VI also show that when the injected noise rate increases, the proposed RCML performs significantly better than the compared methods. Especially under extreme noise rates such as 40% and 50%, RCML achieved in average 22% better  $F_1$  scores and 6% better mAP macro scores than BCE. As an example under 50% injected noise, RCML obtained mAP macro scores almost 30% and 15% higher than SAT and ELR, respectively. Furthermore, we observe that the performance of all the methods does not drop significantly when the injected noise rate is less than 20%. The reason is that the number of clean training samples for each class is still sufficient for the networks to learn and predict them correctly, despite the introduced label noise. The table shows that the mAP micro scores are higher than the mAP macro scores for all the methods. This reveals a class imbalance problem in the IR-BigEarthNet dataset. In this case, the classes with a small number of samples receive below-average scores because macro averaging computes the metric independently for class distributions and then takes the average, whereas micro averaging aggregates the contributions of each class.

For further analysis, we select six representative classes from the IR-BigEarthNet and report their class-based mAP scores in Fig. 7. The class-based mAP scores in Fig. 7 reveal that the proposed RCML and the compared methods learn the classes represented by sufficient training images better than the classes that do not include sufficient number of training images. The classes with a sufficient number of training images (e.g. “Marine waters”) obtain the highest mAP scores under different noise rates. Even high noise rates, such as 40%, do not significantly reduce the mAP scores of these classes. As an example, for class “Marine waters” when the injected noise rate increases from 0% to 40%, RCML and ELR only dropped less than 1% in terms of mAP. The reason is that despite applying high noise rates, the classes with a high number of training images still have many images to learn from. On the other hand, the classes with insufficient training images (e.g., “Urban fabric”, and “Moors, heathland

and sclerophyllous vegetation”) receive a low mAP score over different noise rates. As an example, for class “Urban fabric” when the injected noise rate increases from 0% to 40%, the mAP scores obtained by RCML and SAT dropped about 5% and 25%, respectively. The proposed RCML outperforms the compared methods in the majority of classes, especially under high noise rates, while obtaining comparative or better results compared to the BCE in smaller noise rates (under 20%). In a few classes (e.g., “Arable lands” and “Pasture”), the BCE and RCML performances are comparable over the low rates of the injected label noise. However, by increasing the noise rate, the RCML showed stability and obtained mAP scores higher than the other methods. This demonstrates the robustness of RCML under different variety of injected noise rates.

#### D. Results on Multi-Label UCMerced Dataset

The comparative evaluation results for the multi-label UCMerced dataset are presented in Table VII. By analyzing the results, one can see that increasing the injected noise rates severely affects the learning processes in the multi-label UCMerced dataset. As shown in Table VII, noise creates instability on the compared methods. This is mainly due to the smaller training set of the multi-label UCMerced dataset. In general, the proposed RCML provides relatively stable performance and achieves a degree of robustness against different rates of the label noise. Although the ELR and BCE have achieved comparable mAP micro and mAP macro scores to the proposed RCML under lower noise rates, the RCML could achieve considerably higher mAP as well as  $F_1$  scores under 40% and 50% noise rates. As an example, under 10% injected noise rate BCE obtained 89.5% mAP macro score, marginally better than RCML (0.3% higher). However, when the injected noise rate increases to 40%, the mAP macro score obtained by BCE drops to 74.5%, while the proposed RCML obtained 83.3%. We should note that the ResNet50 is a powerful model capable of tolerating even a relatively high noise rate, but it is not stable under extreme noise rates. Employing the ResNet50 as a classifier within our proposed collaborative framework makes it more stable and robust against higher noise rates. A comparison between Table VI and Table VII reveals that the multi-label UCMerced dataset achieves higher mAP and  $F_1$  scores compared to the IR-BigEarthNet under the same experimental setup. The reason for this is that the features in the images in the multi-label UCMerced dataset are more

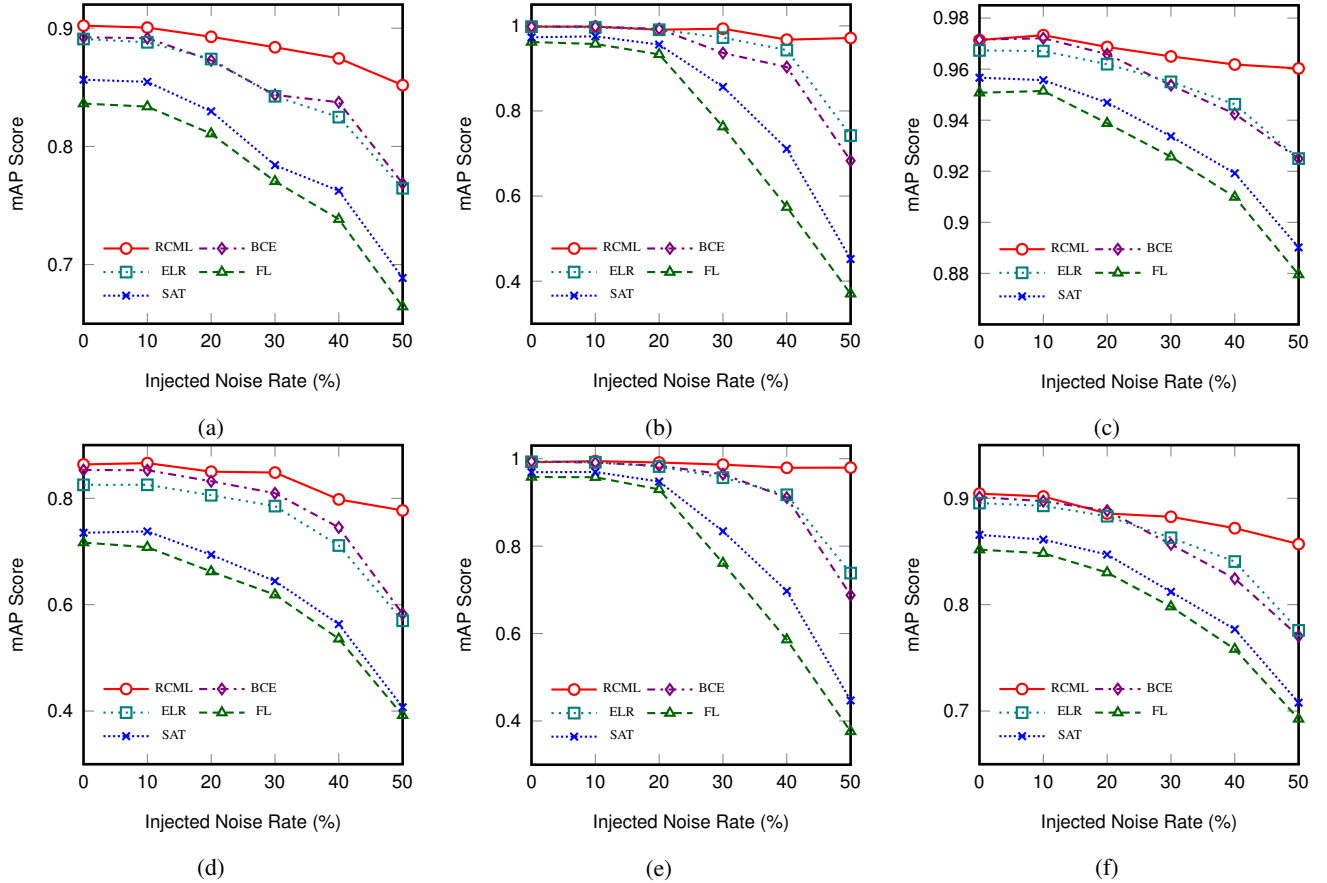


Fig. 8: Class-based comparison: Class-based mAP scores for different noise rates obtained by the proposed RCML, BCE, ELR, FL and SAT for six selected classes: (a) Cars; (b) Dock; (c) Pavement; (d) Sand; (e) Ship; and (f) Trees in the multi-label UCMerced dataset.

similar to the features that are learned in the Imagenet weights. This makes it easier for the classifiers to learn the underlying class distribution from the training set.

Furthermore, we analyzed the class-based performance for the multi-label UCMerced dataset. Fig. 8 shows comparative plots of mAP under different injected noise rates for six representative classes from the multi-label UCMerced dataset. The performance of the compared methods is not stable under different noise rates, as it is shown in Fig. 8. As an example, in the case of the “Dock” class, the mAP scores obtained by the proposed RCML are relatively stable (around 98%), while the compared methods sharply drop when the noise rate exceeds 20% (e.g., ELR and SAT are dropped more than 20% and 45%, respectively). Similar to the IR-BigEarthNet results in Fig. 7, the mAP scores of the classes with a sufficient number of training samples are the highest among the other classes.

## VI. CONCLUSION AND DISCUSSION

In this work, we proposed a robust collaborative multi-label learning (RCML) method to overcome the adverse effects of multi-label noise in the context of scene classification of RS images. The proposed method includes three main modules: 1) discrepancy module; 2) group lasso module; and 3) swap module. The discrepancy module forces the two networks to

learn diverse features while obtaining consistent predictions. The group lasso module detects the individual noisy labels assigned to the training image. By using the group lasso module the RCML method identifies the different multi-label noise types that are associated to missing and wrong class label annotations. Finally, the swap module exchanges the ranking information between two networks and excludes the identified samples associated with noisy labels from the backpropagation dynamically. To the best of our knowledge, RCML is the first method to simultaneously tackle the adverse effects of the two types of multi-label noise without making any prior assumption.

The performance of the proposed method was evaluated under different noise rates trained on two publicly available multi-label benchmark RS image archives. We used the IR-BigEarthNet and the UCMerced archives. The experimental results confirm the effectiveness of the proposed method in specific settings where deterministic label noise is introduced to the multi-label training sets. Furthermore, RCML shows more robustness with respect to the state-of-the-art methods in the presence of high rate label noise such as 30% and more. We would like to point out that developing efficient techniques for handling label noise in multi-label training sets is becoming more and more important. On the one side, due to the increased volume of RS image archives, manual large-



scale image labeling is time-demanding and costly (and thus not fully feasible). On the other side, making use of zero-cost labeling by the use of available thematic products can introduce label noise in the training set. In this context, the proposed RCML is very promising as it allows to identify the potential multi-label noise within the training set without considering any prior assumption. We observe that RCML has identified more than 65% (in average over all noise rates) noisy samples correctly, and by excluding the identified noisy samples from backpropagation could significantly improve the performance of the MCL. Furthermore, the proposed method is intrinsically classifier-independent. Even if in our framework it is implemented in the context of CNNs (because of their efficiency for RS image classification), it can be adapted easily for any other classifier or network architecture.

As a final remark, it is worth noting that the proposed RCML provides more accurate results when the approximated noise rate is close to the injected noise rate in the training set. The noise rate approximation is essential since it determines the swap rate value. As a future work, we plan to extend the proposed RCML to learn the noise rate as an extra parameter during the end-to-end training.

#### ACKNOWLEDGMENTS

This work is funded by the European Research Council (ERC) through the ERC-2017-STG BigEarth Project under Grant 759764 and by the German Ministry for Education and Research as BIFOLD - Berlin Institute for the Foundations of Learning and Data (01IS18025A). The Authors would like to thank Tristan Kreuziger for the valuable discussions during the initial phase of this work.

#### REFERENCES

- [1] L. Bruzzone and B. Demir, "A review of modern approaches to classification of remote sensing data," in *Land Use and Land Cover Mapping in Europe: Practices & Trends*, 1st ed., I. Manakos and M. Braun, Eds. Springer, Dordrecht, 2014, vol. 18, ch. 9, pp. 127–143.
- [2] I. Shendryk, Y. Rist, R. Lucas, P. Thorburn, and C. Ticehurst, "Deep learning - a new approach for multi-label scene classification in planetscope and sentinel-2 imagery," in *IEEE International Geoscience and Remote Sensing Symposium*, Valencia, Spain, 2018, pp. 1116–1119.
- [3] A. Zeggada, F. Melgani, and Y. Bazi, "A deep learning approach to UAV image multilabeling," *IEEE Geoscience and Remote Sensing Letters*, vol. 14, no. 5, pp. 694–698, 2017.
- [4] Y. Hua, L. Mou, and X. X. Zhu, "Recurrently exploring class-wise attention in a hybrid convolutional and bidirectional lstm network for multi-label aerial image classification," *Journal of Photogrammetry and Remote Sensing*, vol. 149, pp. 188–199, 2019.
- [5] A. Alshehri, Y. Bazi, N. Ammour, H. Almubarak, and N. Alajlan, "Deep attention neural network for multi-label classification in unmanned aerial vehicle imagery," *IEEE Access*, vol. 7, pp. 119 873–119 880, 2019.
- [6] G. Sümbül and B. Demir, "A deep multi-attention driven approach for multi-label remote sensing image classification," *IEEE Access*, vol. 8, pp. 95 934–95 946, 2020.
- [7] H. Yessou, G. Sümbül, and B. Demir, "A comparative study of deep learning loss functions for multi-label remote sensing image classification," in *IEEE International Geoscience and Remote Sensing Symposium*, 2020.
- [8] G. Sümbül, M. Charfuelan, B. Demir, and V. Markl, "Bigearthnet: A large-scale benchmark archive for remote sensing image understanding," in *IEEE International Geoscience and Remote Sensing Symposium*, Yokohoma, Japan, 2019, pp. 5901–5904.
- [9] J. Deng, W. Dong, R. Socher, L.-J. Li, K. Li, and L. Fei-Fei, "Imagenet: A large-scale hierarchical image database," in *IEEE Conference on Computer Vision and Pattern Recognition*, Miami, FL, 2009, pp. 248–255.
- [10] G. Büttner, J. Feranec, G. Jaffrain, L. Mari, G. Maucha, and T. Soukup, "The corine land cover 2000 project," *EARSeL eProceedings*, vol. 3, no. 3, pp. 331–346, 2004.
- [11] C. Paris and L. Bruzzone, "A novel approach to the unsupervised extraction of reliable training samples from thematic products," *IEEE Transactions on Geoscience and Remote Sensing*, pp. 1–19, 2020.
- [12] G. Jaffrain, C. Sannier, A. Pennec, and H. Dufourmont, "Corine land cover 2012 - final validation report," European Environment Agency, Tech. Rep., 2017. [Online]. Available: <https://land.copernicus.eu/user-corner/technical-library/clc-2012-validation-report-1>
- [13] H. Jain, Y. Prabhu, and M. Varma, "Extreme multi-label loss functions for recommendation, tagging, ranking & other missing label applications," in *ACM SIGKDD International Conference on Knowledge Discovery and Data Mining*, New York, NY, 2016, pp. 935–944.
- [14] T. Durand, N. Mehrasa, and G. Mori, "Learning a deep convnet for multi-label classification with partial labels," in *IEEE Conference on Computer Vision and Pattern Recognition*, Long Beach, CA, 2019, pp. 647–657.
- [15] T.-Y. Lin, M. Maire, S. Belongie, J. Hays, P. Perona, D. Ramanan, P. Dollár, and C. L. Zitnick, "Microsoft coco: Common objects in context," *European Conference on Computer Vision*, pp. 740–755, 2014.
- [16] C. Zhang, S. Bengio, M. Hardt, B. Recht, and O. Vinyals, "Understanding deep learning requires rethinking generalization," *CoRR*, vol. abs/1611.03530, 2016.
- [17] K. Yi and J. Wu, "Probabilistic end-to-end noise correction for learning with noisy labels," in *IEEE Conference on Computer Vision and Pattern Recognition*, Long Beach, CA, 2019, pp. 7017–7025.
- [18] P. Ulmas and I. Liiv, "Segmentation of satellite imagery using u-net models for land cover classification," *CoRR*, vol. abs/2003.02899, 2020.
- [19] Y. Hua, S. Lobry, L. Mou, D. Tuia, and X. X. Zhu, "Learning multi-label aerial image classification under label noise: A regularization approach using word embeddings," in *IGARSS 2020 IEEE International Geoscience and Remote Sensing Symposium*. IEEE, 2020, pp. 525–528.
- [20] H. Song, M. Kim, D. Park, and J. Lee, "Learning from noisy labels with deep neural networks: A survey," *CoRR*, vol. abs/2007.08199, 2020.
- [21] B. Frenay and M. Verleysen, "Classification in the presence of label noise: A survey," *IEEE Transactions on Neural Networks and Learning Systems*, vol. 25, no. 5, pp. 845–869, 2014.
- [22] A. K. Aksoy, M. Ravanbakhsh, T. Kreuziger, and B. Demir, "A consensual collaborative learning method for remote sensing image classification under noisy multi-labels," in *2021 IEEE International Conference on Image Processing (ICIP)*, 2021, pp. 3842–3846.
- [23] G. Patrini, A. Rozza, A. Krishna Menon, R. Nock, and L. Qu, "Making deep neural networks robust to label noise: A loss correction approach," in *IEEE Conference on Computer Vision and Pattern Recognition*, Long Beach, CA, 2017, pp. 1944–1952.
- [24] J. Goldberger and E. Ben-Reuven, "Training deep neural-networks using a noise adaptation layer," Toulon, France, 2016.
- [25] A. P. Dawid and A. M. Skene, "Maximum likelihood estimation of observer error-rates using the em algorithm," *Journal of the Royal Statistical Society: Series C (Applied Statistics)*, vol. 28, no. 1, pp. 20–28, 1979.
- [26] C. M. Teng, "Evaluating noise correction," in *PRICAI 2000 Topics in Artificial Intelligence*, R. Mizoguchi and J. Slaney, Eds. Berlin, Heidelberg: Springer Berlin Heidelberg, 2000, pp. 188–198.
- [27] H. Noh, T. You, J. Mun, and B. Han, "Regularizing deep neural networks by noise: Its interpretation and optimization," in *Advances in Neural Information Processing Systems*, 2017, pp. 5109–5118.
- [28] S. Liu, J. Niles-Weed, N. Razavian, and C. Fernandez-Granda, "Early-learning regularization prevents memorization of noisy labels," in *Advances in Neural Information Processing Systems*, vol. 33, Vancouver, Canada, 2020.
- [29] S. Sukhbaatar, J. Bruna, M. Paluri, L. Bourdev, and R. Fergus, "Training convolutional networks with noisy labels," in *International Conference on Learning Representations*, San Diego, CA, 2014.
- [30] B. Yuan, J. Chen, W. Zhang, H.-S. Tai, and S. McMains, "Iterative cross learning on noisy labels," in *IEEE Winter Conference on Applications of Computer Vision*, Lake Tahoe, NV, 2018, pp. 757–765.
- [31] M. Dehghani, A. Mehrjou, S. Gouw, J. Kamps, and B. Schölkopf, "Fidelity-weighted learning," in *International Conference on Learning Representations*, Vancouver, Canada, 2017.
- [32] L. Huang, C. Zhang, and H. Zhang, "Self-adaptive training: beyond empirical risk minimization," *Advances in Neural Information Processing Systems*, vol. 33, 2020.
- [33] X. Liu, S. Li, M. Kan, S. Shan, and X. Chen, "Self-error-correcting convolutional neural network for learning with noisy labels," in *IEEE*

- International Conference on Automatic Face & Gesture Recognition*, Washington, DC, 2017, pp. 111–117.
- [34] Z. Hu, K. Gao, X. Zhang, and Z. Dou, “Noise resistant focal loss for object detection,” in *Chinese Conference on Pattern Recognition and Computer Vision (PRCV)*. Springer, 2020, pp. 114–125.
  - [35] T.-Y. Lin, P. Goyal, R. Girshick, K. He, and P. Dollár, “Focal loss for dense object detection,” in *Proceedings of the IEEE international conference on computer vision*, Venice, Italy, 2017, pp. 2980–2988.
  - [36] X. Wu, R. He, Z. Sun, and T. Tan, “A light cnn for deep face representation with noisy labels,” *IEEE Transactions on Information Forensics and Security*, vol. 13, no. 11, pp. 2884–2896, 2018.
  - [37] D. T. Nguyen, T. Ngo, Z. Lou, M. Klar, L. Beggel, and T. Brox, “Robust learning under label noise with iterative noise-filtering,” *CoRR*, vol. abs/1906.00216, 2019.
  - [38] L. Jiang, Z. Zhou, T. Leung, L.-J. Li, and L. Fei-Fei, “Mentornet: Learning data-driven curriculum for very deep neural networks on corrupted labels,” in *International Conference on Machine Learning*, Stockholm, Sweden, 2018, pp. 2304–2313.
  - [39] B. Han, Q. Yao, X. Yu, G. Niu, M. Xu, W. Hu, I. Tsang, and M. Sugiyama, “Co-teaching: Robust training of deep neural networks with extremely noisy labels,” in *Advances in Neural Information Processing Systems*, Montréal, Canada, 2018, pp. 8527–8537.
  - [40] Y. Han, S. Roy, L. Petersson, and M. Harandi, “Learning from noisy labels via discrepant collaborative training,” in *Winter Conference on Applications of Computer Vision*, 2020, pp. 3169–3178.
  - [41] M. Ren, W. Zeng, B. Yang, and R. Urtasun, “Learning to reweight examples for robust deep learning,” *CoRR*, vol. abs/1803.09050, 2018.
  - [42] A. Ghosh, H. Kumar, and P. S. Sastry, “Robust loss functions under label noise for deep neural networks,” in *Proceedings of the Thirty-First AAAI Conference on Artificial Intelligence*, 2017, p. 1919–1925.
  - [43] Z. Zhang and M. Sabuncu, “Generalized cross entropy loss for training deep neural networks with noisy labels,” in *Advances in Neural Information Processing Systems*, Montréal, Canada, 2018, pp. 8778–8788.
  - [44] J. Li, Y. Wong, Q. Zhao, and M. S. Kankanhalli, “Learning to learn from noisy labeled data,” in *IEEE Conference on Computer Vision and Pattern Recognition*, Long Beach, CA, 2019, pp. 5051–5059.
  - [45] S. S. Bucak, R. Jin, and A. K. Jain, “Multi-label learning with incomplete class assignments,” in *IEEE Conference on Computer Vision and Pattern Recognition*, Colorado Springs, CO, 2011, pp. 2801–2808.
  - [46] M. Yuan and Y. Lin, “Model selection and estimation in regression with grouped variables,” *Journal of the Royal Statistical Society: Series B (Statistical Methodology)*, vol. 68, no. 1, pp. 49–67, 2006.
  - [47] A. Blum and T. Mitchell, “Combining labeled and unlabeled data with co-training,” in *Conference on Computational Learning Theory*, New York, NY, 1998, pp. 92–100.
  - [48] A. Gretton, K. M. Borgwardt, M. J. Rasch, B. Schölkopf, and A. Smola, “A kernel two-sample test,” *The Journal of Machine Learning Research*, vol. 13, no. 1, pp. 723–773, 2012.
  - [49] S. Vallender, “Calculation of the wasserstein distance between probability distributions on the line,” *Theory of Probability & Its Applications*, vol. 18, no. 4, pp. 784–786, 1974.
  - [50] M. A. Alvarez, L. Rosasco, and N. D. Lawrence, “Kernels for vector-valued functions: A review,” *arXiv preprint arXiv:1106.6251*, 2011.
  - [51] J.-P. Vert, K. Tsuda, and B. Schölkopf, “A primer on kernel methods,” *Kernel Methods in Computational Biology*, vol. 47, pp. 35–70, 2004.
  - [52] G. Sumbul, A. d. Wall, T. Kreuziger, F. Marcelino, H. Costa, P. Benevides, M. Caetano, B. Demir, and V. Markl, “Bigearthnet-mm: A large scale multi-modal multi-label benchmark archive for remote sensing image classification and retrieval,” *IEEE Geoscience and Remote Sensing Magazine*, vol. 9, no. 3, pp. 174–180, Sept. 2021.
  - [53] Y. Yang and S. Newsam, “Bag-of-visual-words and spatial extensions for land-use classification,” in *SIGSPATIAL International Conference on Advances in Geographic Information Systems*, New York, NY, 2010, pp. 270–279.
  - [54] B. Chaudhuri, B. Demir, S. Chaudhuri, and L. Bruzzone, “Multilabel remote sensing image retrieval using a semisupervised graph-theoretic method,” *Transactions on Geoscience and Remote Sensing*, vol. 56, no. 2, pp. 1144–1158, 2018.
  - [55] K. He, X. Zhang, S. Ren, and J. Sun, “Deep residual learning for image recognition,” in *IEEE Conference on Computer Vision and Pattern Recognition*, 2016, pp. 770–778.
  - [56] K. He, X. Zhang, S. Ren, and S. Jian, “Identity mappings in deep residual networks,” in *European Conference on Computer Vision*. Las Vegas, NV: Springer, 2016, pp. 630–645.